

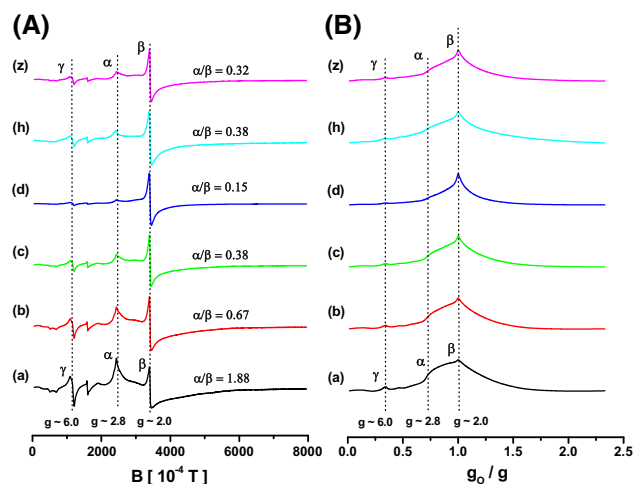
‘U-spectrum’ type of Gd(III) EPR spectra recorded at various stages of TEOS-based sol–gel process

Milan Mazur¹ · Patrik Poprac¹ · Marian Valko¹ · Christopher J. Rhodes²

Received: 12 January 2016 / Accepted: 12 March 2016 / Published online: 21 March 2016
© Springer Science+Business Media New York 2016

Abstract The various stages of the tetraethyl orthosilicate-based sol–gel process were studied using Gd(III) cations as a spin probe, using EPR spectroscopy at ambient and liquid nitrogen temperatures. The Gd(III) EPR spectra (being of the ‘U-spectrum’ type) were very similar, as recorded at 77 K, at the various defined stages of the sol–gel process. The analysis of the experimental EPR spectra showed that as the sol–gel process proceeded, the spin Hamiltonian parameters remained unchanged, but the relative amplitude of the α -line (at $g \sim 2.8$) and β -line (at $g \sim 2.0$) changed significantly, such that the α/β -ratio decreased progressively. This is the first report that the silica sol-to-gel transition from the low viscosity, starting reaction mixture, to the high viscosity, colloid suspension, up to the viscoelastic gel and finally to the dry gel, can be successfully monitored using Gd(III) EPR spectroscopy.

Graphical Abstract



Keywords Sol–gel process · TEOS · EPR spectroscopy · Spin probe · Gd(III) cations

1 Introduction

EPR spectroscopy is a powerful technique for the provision of useful information regarding structural details of the environment of both transition metal ions and rare-earth ions in glasses, such as their coordination number, valence state, local symmetry, charge compensation and the degree of short range disorder [1]. There is, nonetheless, a paucity of such measurements on rare-earth ions in glassy solids, in comparison with transition metal ions in similar media [2].

Vitreous materials play an important role in various contemporary technologies [1]. Glasses doped with rare-

✉ Milan Mazur
milan.mazur@stuba.sk

¹ Faculty of Chemical and Food Technology, Slovak Technical University, Radlinskeho 9, 812 37 Bratislava, Slovakia

² School of Chemistry, University of Reading, Reading, UK

earth elements are especially important in various optical and optoelectronic devices [3], e.g., gadolinium-containing glasses, which have particular optical and magnetic properties to render them suitable for a wide range of technological applications in optical communications, laser technology and optical storage devices [1].

EPR spectra obtained from both glassy materials and disordered polycrystalline materials, containing gadolinium, have been analyzed by many authors [1–20]. To the best of our knowledge, however, no EPR studies have been reported of structural changes that occur in the various stages of the silica sol–gel process using Gd(III) ions as a spin probe until now, apart from the EPR study of Gd(III) complexes immobilized in a silica xerogel matrix as presented by Szyzewski et al. [21]. However, the sol–gel glasses have numerous advantages over melt glasses, in particular, a higher purity of the starting materials, lower processing temperatures, that they may be produced by simple chemical manipulation techniques, a greater homogeneity and precision control of the chemical composition of the final products [22].

The X-band EPR spectra of Gd(III) ions present at low concentrations in almost any type of glassy host tend to be very similar and are characterized by three prominent features with effective g values of ~ 2.0 , ~ 2.8 and ~ 6.0 [7]. This type of Gd(III) EPR spectrum has been aptly labeled the ‘U-spectrum’ [6], in view of its ‘ubiquity’ in various glassy and disordered polycrystalline materials [1–20]. Less frequently, X-band EPR ‘U-spectra’ with additional weak features at effective g values of ~ 3.3 to ~ 3.6 and/or ~ 4.3 to ~ 4.8 are observed from Gd(III) ions in glasses [1, 3, 12–18].

The origin of the ‘U-spectrum’ of Gd(III) ions in glasses has been interpreted differently by different authors [4–10]. An exact analysis of the Gd(III) EPR ‘U-spectrum’ is a complicated matter and has been the subject of considerable controversy [12].

Having made a systematic evaluation of the various published interpretations of Gd(III) EPR ‘U-spectra’ [4, 5, 9, 10] and found all of them to be unsatisfactory, Brodbeck and Iton [11] managed to establish the correct general solution of the Gd(III) EPR spectra in glassy and disordered polycrystalline materials. Based on the $\mathbf{H}_{\text{CF}}/h\nu$ ratio (where \mathbf{H}_{CF} is crystal field interaction, h is Planck’s constant, and ν is microwave frequency), the Gd(III) EPR spectra can be divided into three crystal field categories: weak, intermediate and strong. In the weak crystal field category, $\mathbf{H}_{\text{CF}}/h\nu \leq 1/4$ (including the weak crystal field limit), the EPR spectrum arises primarily from first-order transitions between the Zeeman levels which are only weakly perturbed by \mathbf{H}_{CF} . Higher-order transitions with $g > 2.0$ are strongly forbidden due to the weak \mathbf{H}_{CF} , and the spectrum is principally concentrated in the region of $g = 2.0$. In the intermediate crystal field category,

$1/4 \leq \mathbf{H}_{\text{CF}}/h\nu \leq 4$ (which is further divided into two parts), the EPR spectrum generally consists of multiple resonances, the majority of which have effective g values > 2.0 . In the case of lower intermediate crystal field strength, $1/4 \leq \mathbf{H}_{\text{CF}}/h\nu \leq 1$, the EPR spectrum may consist of a wide dispersion of resonances throughout the entire range of $2.0 \leq g \leq \infty$. In the case of upper intermediate crystal field strength, $1/4 \leq \mathbf{H}_{\text{CF}}/h\nu \leq 4$, the ER spectrum is focused on a smaller set of resonances with $g > 2.0$, as the number of transitions that can occur between the Kramers levels is reduced. In the strong crystal field category, $\mathbf{H}_{\text{CF}}/h\nu \geq 4$ (including the strong crystal field limit), the EPR spectrum is entirely determined by those few resonances resulting from transitions within the Kramers’ levels [11]. Clearly, the Gd(III) EPR spectra must vary strongly with the microwave frequency within the range of 5.4–38.4 GHz. At the upper limit of the range, which is the Q-band frequency, the widely dispersed resonances detected at X-band are observed to coalesce into a single prominent $g = 2.0$ feature, because of the increase in $h\nu$ by a factor of 4 [11]. Furthermore, it was concluded that the ‘U-spectrum’ is expected to prevail only when the Gd(III) ions can achieve a high coordination number (≥ 6) within the structurally disordered matrixes. Thus, the site symmetries of the Gd(III) ions are essentially low and disordered which dictate their own environment in glasses and are best characterized by a single low-symmetry-type site, as was proposed by Griscom [8].

From the point of view of EPR spectroscopy, the silica sol–gel process may be regarded as proceeding via a progression of steps as shown in Fig. 1 of Ref. [23]: (a) the initial reaction mixture which is in the form of a fluid, water-like solution; (b) the colloidal suspension (sol) which is in a highly viscous liquid state; (c) the sample in which rigid boundaries of the solid state are visible, i.e., a wet gel (a viscoelastic solid state); and (d) the gel after being dried (dry gel), which is a rigid solid that can be powdered. In our previous papers [23–25], we monitored the earlier stages of the tetraethyl orthosilicate (TEOS)-based sol–gel process, and we determined the changes in the properties of the sol–gel reaction mixture, as it passes from the liquid state to the solid state, using EPR spectroscopy with the transition metal ions, Mn(II), VO(II) and Cu(II), as a spin probe. The object of the present paper is to further determine the defined stages of the TEOS-based sol–gel process, but using EPR spectroscopy with the rare-earth ion, Gd(III), as a spin probe.

2 Experimental

The commercially available chemicals, TEOS (Sigma-Aldrich, 98.0 %), ethanol for UV (MicroChem), HCl (MicroChem) and GdCl₃·H₂O (Sigma-Aldrich, 98.0 %),

were used without further purification. The identical procedure for preparation of the sol–gel samples was employed as described in our previous paper [23]. Very briefly: In the present study, the Gd(III) ions (concentration ca 1 mM) were incorporated in the form of the $\text{GdCl}_3 \cdot \text{H}_2\text{O}$ into the binary mixture (TEOS, ethanol) before hydrolysis began. Then, re-distilled water containing HCl was added dropwise to catalyze the hydrolysis. Under the following conditions (in air at RT, and in closed containers with a plastic cover with holes in it), the gelation was completed after about 2 weeks giving a wet gel, which was then dried (in air at 100 °C for 12 h) giving a dry gel. The EPR spectra were measured during the evolution of the sol–gel process at the times defined (immediately, then hourly, up to 12 h, and then daily, up to 30 days), additionally, in the dry gel sample, which was hydrated by storing them for 3 days in a container with an atmosphere saturated with water vapor at RT, and for the sol–gel process as run in a sealed quartz EPR capillary. As a brief summary, the Gd(III) EPR spectra (with a central field of 4000×10^{-4} T and a sweep width of 8000×10^{-4} T) were recorded using an EMX series Bruker EPR spectrometer at room temperature (RT) and at 77 K. Quartz EPR sample tubes were precisely positioned in the microwave cavity using our special procedure [26, 27]. The processing, simulation and evaluation of the EPR spectra were performed as described in our previous papers in this series [23–25, 28]. Again, very briefly: The spin Hamiltonian parameter values were determined from experimental Gd(III) EPR spectra using original Bruker program WinEPR [29]. Then, these values were further refined by computer simulations using original Bruker program SimFonia [30], which allows the simulation of the EPR spectra in the solutions, frozen solutions as well as in the solid state using an efficient perturbation theory (the second or the third order) algorithm. No EPR signal was obtained from the control sample in which Gd(III) ions were absent.

3 Interpretation and simulation of Gd(III) EPR spectra

The Gd(III) ion has an electronic configuration of $4f^7$, a ground-state term of $^8S_{7/2}$ and a spin quantum number, $S = 7/2$ [31]. In accordance with Abragam and Bleaney [32], we have described the EPR spectrum of Gd(III) in the solid state using a spin Hamiltonian, which contains only those terms which correspond to the electronic Zeeman interaction (\mathbf{H}_Z) and the crystal field interaction (\mathbf{H}_{CF}). It is assumed that the hyperfine interaction term (with an orbital angular momentum, $L = 0$) and other smaller terms can be neglected [6], in which case,

$$\mathbf{H} = \mathbf{H}_Z + \mathbf{H}_{CF} \quad (1)$$

The operators can generally be written for Gd(III) ions in the following way [33],

$$H = g_0 \beta B S + D \left\{ S_z^2 - \frac{1}{3} S(S+1) \right\} + E (S_x^2 - S_y^2) \quad (2)$$

where g_0 is equal to the isotropic, free electron g value, β is the Bohr magneton, B is the applied external magnetic field intensity, S is the spin angular momentum, and D and E are the zero-field splitting parameters.

As mentioned in Sect. 1, Brodbeck and Iton [11] concluded that the X-band EPR spectra of S-state Gd(III) ions, as are present at low concentrations in glassy materials, show three main features with effective g factor values of ~ 2.0 , ~ 2.8 and ~ 6.0 and are referred to as the ‘U-spectrum’ because of the ‘ubiquity’ of this spectral form in various disordered materials [6]. The features of such ‘U-spectrum’ are highly sensitive to changes in the zero-field splitting parameter D and E/D-ratio [2, 6, 7, 11]. We have computer-simulated Gd(III) EPR ‘U-spectra,’ which were calculated for various D values in the range of $0.020\text{--}0.070 \text{ cm}^{-1}$ (Fig. 1a) and various E/D-ratios in the range of $0.00\text{--}0.30$ (Fig. 1b). It is clear that the position of the central resonance with $m_S = \pm 1/2$ on the magnetic field strength axis is practically independent of an increase in the D value. In contrast, those resonance lines with $m_S = -3/2$ and $-5/2$ and especially with $m_S = -7/2$ are progressively shifted toward lower magnetic field strengths. This is true also for those resonance lines with $m_S = 3/2$ and $5/2$ and particularly with $m_S = 7/2$, but they are progressively shifted toward higher magnetic field values. However, the resonance positions of the corresponding lines on the magnetic field strength axis are practically independent of the E/D-ratio (except for that of 0.30) for all values of m_S . Additionally, the shape of a pronounced ‘valley’ exhibited in the region of $m_S = -3/2$ and $m_S = \pm 1/2$ of the ‘U-spectrum’ changes appreciably as the D value and E/D-ratio increases.

4 Results and discussion

Figure 2 shows the representative, experimental (A) first-derivative and (B) absorption Gd(III) EPR spectra measured at liquid nitrogen temperature (77 K) for the various stages ($a\text{--}d$) of the sol–gel process, hydrated dry gel (h) and sol–gel processed in the sealed capillary (z). The first-derivative EPR spectra are plotted versus external magnetic field strength, \mathbf{B} , but the absorption spectra are plotted versus the g_0/g -ratio. The effective g factor values, α , β , γ resonance lines and α/β -ratio are indicated for better representation in the spectra. Then, Fig. 3 illustrates the

Fig. 1 Simulated first-derivative Gd(III) EPR spectra computed for **a** various values of the zero-field splitting parameter, D (0.020–0.070) cm^{-1} and **b** various values of the E/D -ratio (0.00–0.30). The m_S values ($\pm 7/2$, $\pm 5/2$, $\pm 3/2$, $\pm 1/2$) are indicated

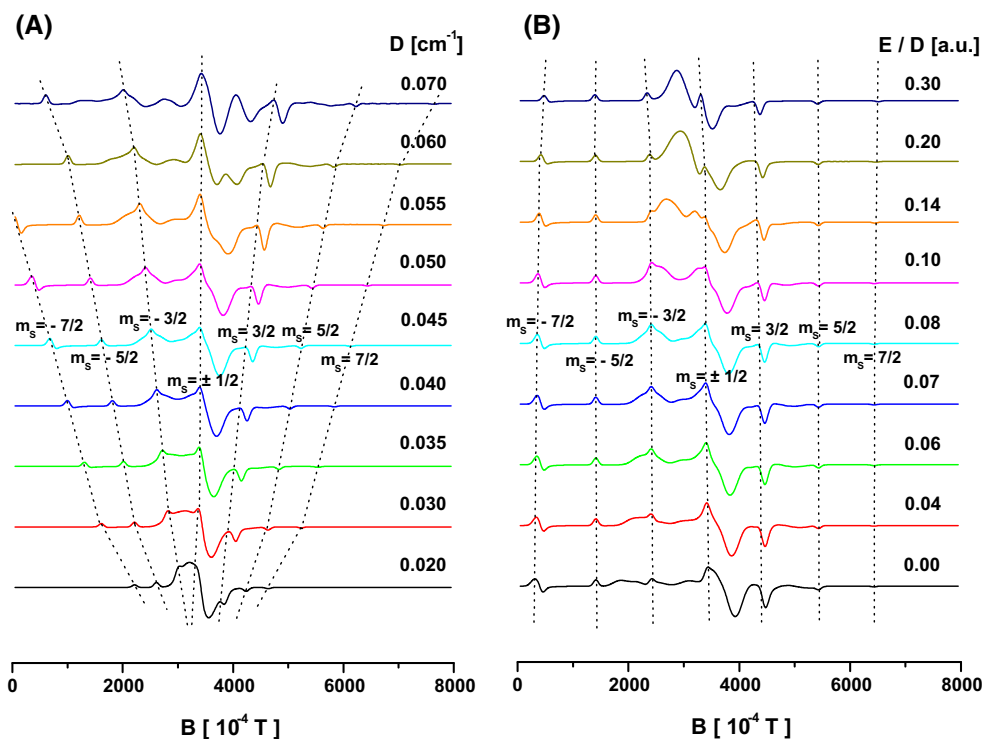
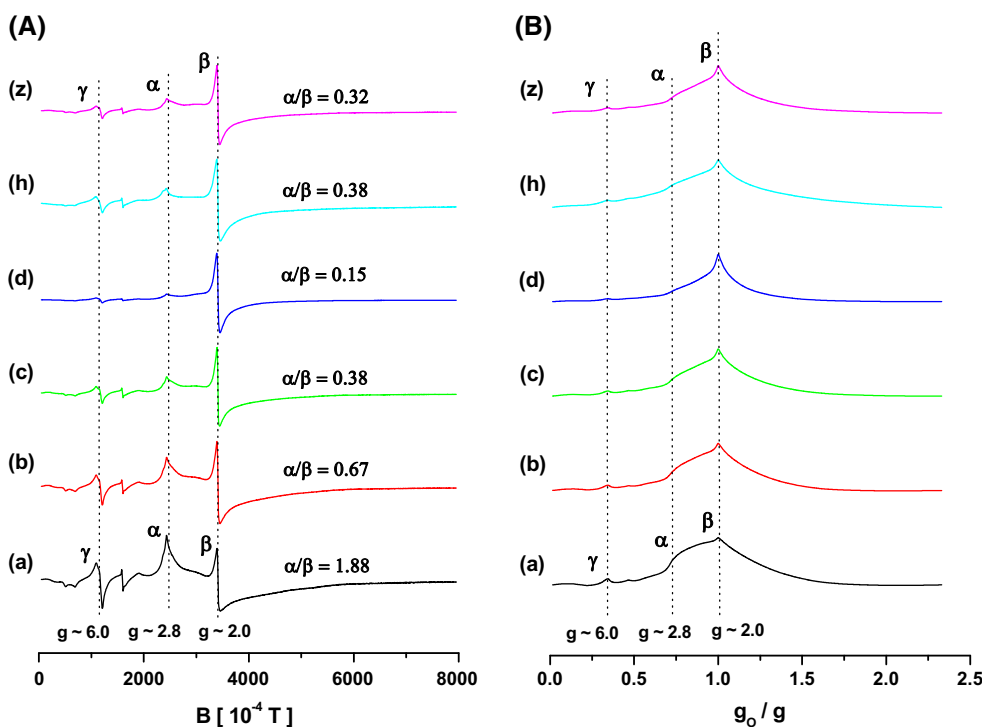


Fig. 2 Experimental, **A** first-derivative and **B** absorption Gd(III) EPR spectra measured at 77 K for the various stages of the sol–gel process: (a) reaction mixture (solution of low viscosity), (b) sol (colloidal suspension, solution of high viscosity), (c) wet gel (viscoelastic solid), (d) dry gel (powder solid state), (h) hydrated dry gel and (z) process occurring in a sealed capillary. Absorption EPR spectra are plotted versus g_0/g -ratio. Effective g -factors, α , β , γ lines and α/β -ratio are indicated



details of **(A)** the low field part ($m_S = -7/2, -5/2$), **(B)** the middle field part ($m_S = -3/2, \pm 1/2$) and **(C)** the high field part ($m_S = 3/2, 5/2, 7/2$) of the first-derivative Gd(III) EPR spectra, which are shown in Fig. 2A.

All the observed first-derivative X-band Gd(III) EPR spectra exhibit three prominent resonance signals at effective g values of 1.99 ± 0.01 (β -line), 2.78 ± 0.01 (α -line) and 5.99 ± 0.01 (γ -line), superimposed on a broad

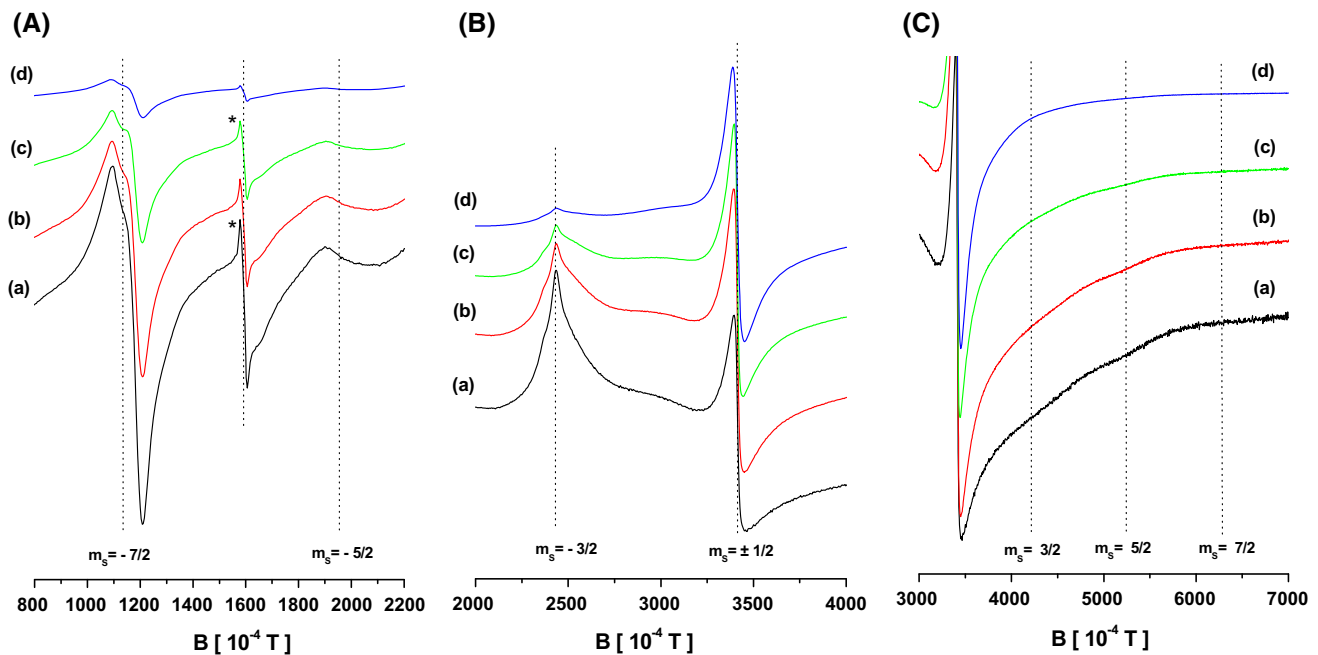


Fig. 3 Expansion of **A** low ($m_S = -7/2, -5/2$), **B** middle ($m_S = -3/2, \pm 1/2$) and **C** high ($m_S = 3/2, 5/2, 7/2$) field part of experimental first-derivative Gd(III) EPR spectra (shown in Fig. 2A)

resonance line shape that encompasses the prominent $g \sim 2.0$ resonance signal, which is a characteristic signature of the typical ‘U-spectrum’ of Gd(III) ions contained in the glassy hosts. There is also a pronounced valley in the line shape beginning at $g = 2.78$ and extending out to $g = 1.99$. Additionally, two weak broad signals at effective g values of 3.46 ± 0.01 and $g = 4.33 \pm 0.01$ were observed. Significant resonance signals are also present at effective g values of 10.49 ± 0.01 , 14.45 ± 0.01 and 29.99 ± 0.01 . The small, sharp line that is present in the spectra of Figs. 2A and 3A (*-marked) at $g = 4.29 \pm 0.01$, and superimposed on the broad line in the $g = 4.33 \pm 0.01$ region, is due to a low concentration of Fe(III) ions, present as an impurity, and is not connected with the Gd(III) EPR spectra. However, this sharp resonance served to provide an internal g value marker for a preliminary determination of the effective g values in the latter, which were further refined by subsequent computer simulation. At the low concentrations of Gd(III) ions (ca 1 mM) used, no EPR spectral shape was observed which would indicate the presence of gadolinium clusters, and hence, we may conclude that the Gd(III) ions are present as isolated species randomly distributed in the sol–gel products [1–3, 7, 11–20, 38, 39].

Within experimental error, the corresponding effective g factor values were found to be identical for all the cases (a – d , h , z), albeit that the relative amplitudes of the two central lines (α and β) do depend on the stage that the sol–gel process is at. For example, in the reaction mixture (a), the α -line is

more intense, while in the wet gel (c) and dry gel (d), the β -line is dominant (see Fig. 2A). Accordingly, the α/β -ratio was varied significantly as the sol–gel process advanced, with a maximal value of 1.88 ± 0.03 being obtained in the reaction mixture (a), 0.67 ± 0.03 in the sol (b), 0.38 ± 0.03 in the wet gel (c) and a minimal value of 0.15 ± 0.03 in the dry gel (d). The α/β -ratio value of 0.38 ± 0.03 , which was obtained in the hydrated dry gel sample (h), is identical with that observed in the wet gel (c): The value of 0.29 ± 0.03 obtained for sol–gel process as carried out in the sealed capillary (z) is very similar. The same trend was seen for the γ/β -ratio with a maximal value of 0.76 ± 0.03 in the reaction mixture (a), 0.28 ± 0.03 in the sol (b), 0.17 ± 0.03 in the wet gel (c) and a minimal value of 0.06 ± 0.03 in the dry gel (d). Once more, the values obtained for the hydrated dry gel (h), 0.19 ± 0.03 , and sol–gel process occurring in the sealed capillary (z), 0.13 ± 0.03 , are very similar to those observed for the wet gel (c). Thus, changes in the sol–gel mixture may be monitored successfully using either the α/β -ratio or the γ/β -ratio; in contrast, within experimental error, the γ/α -ratio value of 0.43 ± 0.03 was found to be identical for all cases (a – d , h , z). This is the first report that the silica sol-to-gel transition from the low viscosity, starting reaction mixture (a), to the high viscosity, colloid suspension (b), up to the viscoelastic gel (c) and finally to the dry gel (d), can be successfully monitored using Gd(III) EPR spectroscopy. In near future, the silica xerogels calcined at various temperatures will be analyzed by EPR spectroscopy using Gd(III) ions as a spin probe.

We may conclude that the Gd(III) EPR spectra measured in this work fulfilled all the points which were ascribed by Brodbeck and Iton [11] for ‘U-spectra’: (i) The $g = 2.78$ (α -line) and 5.99 (γ -line) features always appear jointly, exhibiting approximately the same amplitudes and shape relative to each other (see Fig. 2A); (ii) the feature at $g = 1.99$ (β -line) has a first-derivative amplitude and shape that varies from stage to stage of the sol–gel process, as can be seen by comparing the relative amplitudes of the $g = 1.99, 2.78$ and 5.99 features in Fig. 2A; and (iii) the ‘U-spectrum’ adsorption curve has significant absorptions dispersed throughout the low field region $1.99 \leq g \leq \infty$ (see Figs. 2A, B).

A comparison of the selected experimental first-derivative Gd(III) EPR spectrum versus calculated EPR spectrum separately for (A) the low field part $(800\text{--}2000) \times 10^{-4}$ T, (B) the middle field part $(2000\text{--}4000) \times 10^{-4}$ T and (C) the high field part $(4000\text{--}8000) \times 10^{-4}$ T, is shown in Fig. 4, where the corresponding m_S values ($\pm 7/2, \pm 5/2, \pm 3/2, \pm 1/2$) are again indicated. As was confirmed by computer simulation (see Fig. 1), the features of the Gd(III) EPR ‘U-spectrum’ are highly sensitive to changes in the values of the zero-field splitting parameter D and the E/D-ratio. The best agreement between the computed and experimental Gd(III) EPR spectra was obtained by using $D = 0.051 \text{ cm}^{-1}$ and $E/D = 0.069$ with a line width, $\Delta B = 250$ G, which are in accord with those reported in the literature [2, 6–8, 11, 19, 34–37] glassy systems doped with Gd(III) ions.

The first-derivative Gd(III) EPR spectra, which were measured at ambient temperature (RT), exhibited identical features in all cases (a – d , h , z). The typical line shape of such Gd(III) EPR spectra together with the computer-simulated EPR spectrum is illustrated in Fig. 5, and the corresponding effective g factor values and α , β , γ resonance lines are indicated in both spectra. The overall shape of the Gd(III) EPR spectrum was found to change dramatically for all the given samples when they were measured at RT, from that recorded at 77 K. Nonetheless, the experimental Gd(III) EPR spectrum in Fig. 5 still presents the three characteristic and prominent resonance signals at effective g values of 1.99 (β -line), 2.78 (α -line) and 5.99 (γ -line), which are superimposed on a broad resonance line shape at $g \sim 2.0$, although the additional signals at effective g values of 3.46 and 4.33 were not resolved. It is noteworthy that the EPR spectral lines at RT are much broader than those recorded at 77 K. The good fit of the calculated-to-experimental RT EPR spectrum was obtained by increasing the line width to $\Delta B = 380$ G. This result is in accord with those of Iton and Turkevich [6], in which at RT virtually all of the resonance intensity is present in a broad ($\Delta B = 350$ G), and fairly symmetric feature centered at $g = 1.99$; additional lines were detected at low field, but these comprise only very minor features of the overall

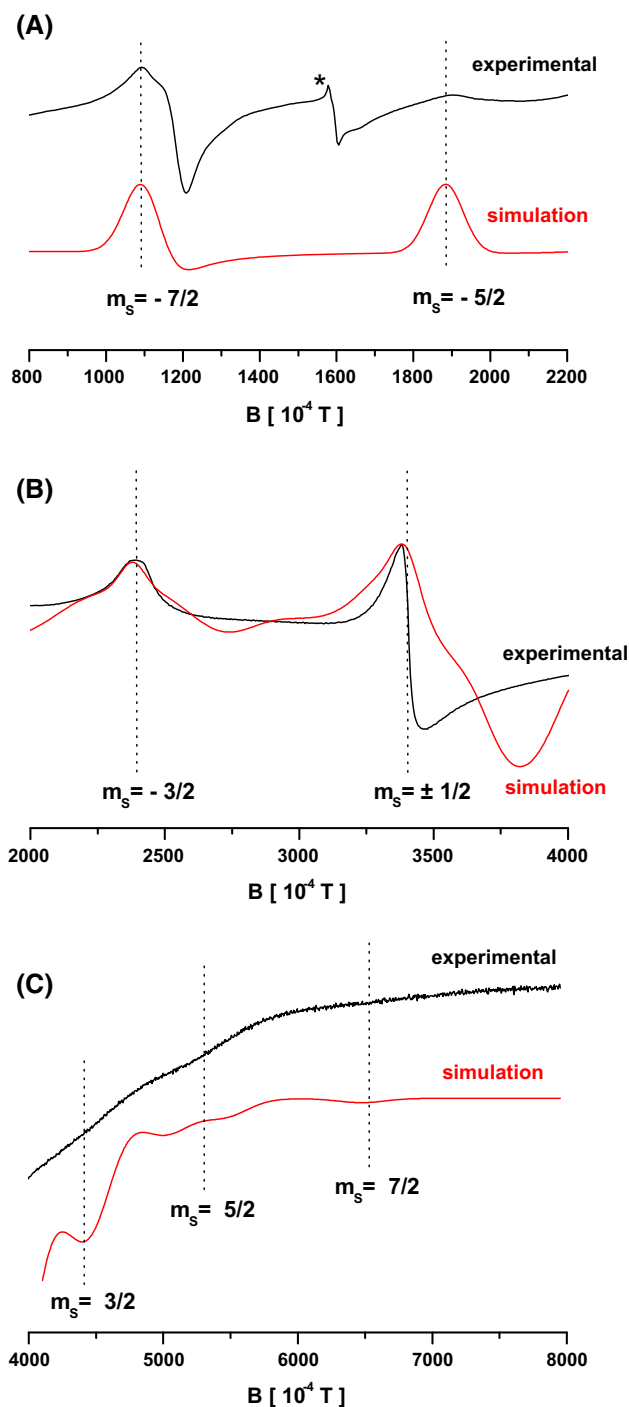


Fig. 4 Illustration of experimental versus simulated **a** low $(800\text{--}2000) \times 10^{-4}$ T, **b** middle $(2000\text{--}4000) \times 10^{-4}$ T and **c** high $(4000\text{--}8000) \times 10^{-4}$ T field part of the first-derivative Gd(III) EPR spectrum. The m_S values ($\pm 7/2, \pm 5/2, \pm 3/2, \pm 1/2$) are indicated

spectrum. In the water solutions, the Gd(III) ions are present in the form of $[\text{Gd}(\text{H}_2\text{O})_8]^{3+}$ complexes [40], and at RT these solvated gadolinium ions undergo free tumbling. The line broadening at RT may thus be a result of spin relaxation effects induced by a rapid tumbling motion of

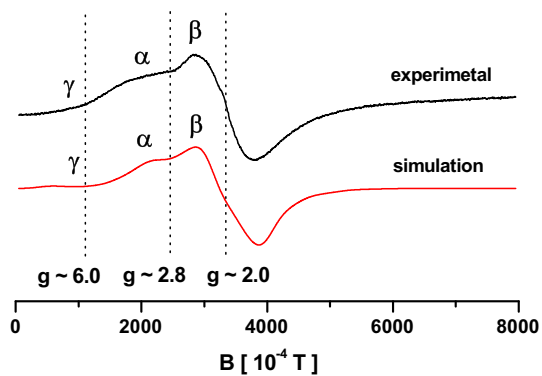


Fig. 5 Identical line shape of experimental first-derivative Gd(III) EPR spectra as obtained at RT for all the stages of the sol–gel process and corresponding simulated first-derivative Gd(III) EPR spectrum. Effective g -factors and α , β , γ lines are indicated

the ions, to yield a single, uninformative resonance near $g \sim 2.0$ [33].

In 1980, Griscom [8] proposed that the Gd(III) ions tend to dictate their own environments when present in glass systems as impurities and hence should be described by single low-symmetry glassy-type sites characterized by a quite broad distribution of crystal fields. This hypothesis was largely confirmed in 1985 by Iton and Brodbeck [11] and further supported by the very similar spectral features, which are found in the EPR spectra of Gd(III) ions in the different glasses [1, 3, 12–20, 34–39]. It is the majority view [3, 12–17, 38, 39] that the lines of ‘U-spectrum’ with effective g values of ~ 2.0 , ~ 2.8 and ~ 6.0 can be assigned to Gd(III) ions with coordination numbers greater than six, while those lines with g values of ~ 3.3 to ~ 3.6 and/or ~ 4.3 to ~ 4.8 might be associated with some Gd(III) ions with coordination numbers of less than six. Resonances corresponding to the above-listed g values are typically found in both vitreous materials and disordered polycrystalline materials [1, 3, 12–20, 34–39]. In tetrahedral network glasses such as silicates, the Gd(III) ions can function as network modifying ions.

While it is the general view that Gd(III) ions can dictate their own environments and occupy sites surrounded by polyhedra of more or less irregularly distributed ligands with high coordination numbers higher than six, in glassy systems, contrastingly, transition metal ions [e.g., Ti(III), Co(II), Ni(II), Fe(III), Mn(II), VO(II) and Cu(II)] are generally localized in sites with octahedral coordination geometries in such media [2, 3, 7, 13, 23–25].

5 Conclusions

Very similar 77 K Gd(III) EPR spectra (‘U-spectrum’ type) were recorded at the various defined stages of the TEOS-based sol–gel process. Analysis of the experimental EPR

spectra showed that as the sol–gel transformation proceeded, the spin Hamiltonian parameters remained unchanged (within experimental error), but the relative amplitudes of the β -line (at $g \sim 2.0$) and the α -line (at $g \sim 2.8$) changed significantly, such that the α/β -ratio decreased progressively throughout the process. Accordingly, those changes that occurred in the sol–gel reaction mixture during its liquid-state to solid-state transformation could be monitored on the basis of the changing α/β -ratio. This is the first report of the sol-to-gel transformation, in the silica sol–gel process, being successfully monitored using EPR spectroscopy with Gd(III) ions as a spin probe.

Acknowledgments This work was supported by the Scientific Grant Agency of the Slovak Republic (Projects VEGA 1/0765/14 and 1/0041/15).

References

- Pascuta P, Culea E (2012) *J Mater Sci* 47:2345–2351
- Wong J, Angel C (1976) *Glass structure by spectroscopy*. Marcel Dekker, Basel
- Srinivasulu K, Omkaram I, Obeid H, Kumar AS, Rao JL (2013) *J Mol Struct* 1036:63–70
- Nicklin RC, Johnstone JK, Barnes RG, Wilder DR (1973) *J Chem Phys* 59:1652–1668
- Chepeleva IV, Lazurkin VN (1976) *Dokl Akad Nauk SSSR* 226:311–318 (in Russian)
- Iton LE, Turkevich J (1977) *J Phys Chem* 81:435–449
- Griscom DL (1990) *Electron spin resonance*. In: Uhlmann DR, Kreidl NJ (eds) *Glass: science and technology*, vol 4B. Academic Press, Boston
- Griscom DL (1980) *ESR in glasses*. *J Non-Cryst Solids* 40:211–272
- Cugunov L, Kliava J (1982) *J Phys C Solid State Phys* 15:L933–L936
- Koopmans HJA, Perik MMA, Nieuwenhuijse B, Gellings PJ (1983) *Phys Status Solidi B* 120:745–751
- Brodbeck CM, Iton LE (1985) *J Chem Phys* 83:4285–4299
- Venkatasubbaiah A, Sreedhar B, Rao JL, Lakshman SVJ, Kojima K (1994) *Mater Res Bull* 29:911–917
- Sreedhar B, Sumalatha Ch, Kojima K (1995) *J Non-Cryst Solids* 192&193:203–206
- Rada M, Culea E, Rada S, Pascuta P, Culea M, Dan V, Rusu T, Maties V, Bratu I (2009) *J Phys Struct* 182:1–4
- Rada S, Culea E, Rada M (2011) *Mater Chem Phys* 128:464–469
- Dehelean A, Rada S, Popa A, Culea E (2013) *J Mol Struct* 1036:203–208
- Zagarai M, Rus L, Rada S, Stan S, Rada M, Bolundut L, Pica ME, Culea E (2014) *J Non-Cryst Solids* 405:129–134
- Murali A, Chakradhar RPS, Rao JL (2005) *Phys B* 364:142–149
- Azzoni CB, Martino DD, Paleari A, Speghini A, Bettinelli M (1999) *J Mater Sci* 34:3931–3935
- Kliava J, Malakhovskii A, Zarubina T, Petrovskii G (2005) *Phys Rev B* 71:104406–104409
- Szyczewski A, Lis S, Krzystek J, Staninski K, Klonekowski A, Kruczyński Z, Pietraszkiewicz M (2008) *J Alloys Compd* 451:182–185
- Brinker CJ, Scherer GW (1990) *Sol–gel science*. Academic Press, New York
- Mazur M, Kleinová M, Moncol J, Stachová P, Valko M, Telser J (2006) *J Non-Cryst Solids* 352:3158–3165

24. Mazur M, Husáriková L, Rhodes CJ, Valko M (2015) *J Sol-Gel Sci Technol* 76:110–119
25. Mazur M, Husáriková L, Valko M, Rhodes CJ (2016) *Appl Magn Reson* 47:1–12
26. Mazur M, Valko M, Klement R, Morris H (1996) *Anal Chim Acta* 333:249–252
27. Mazur M, Valko M, Morris H, Klement R (1996) *Anal Chim Acta* 333:253–265
28. Pelikán P, Liška M, Valko M, Mazur M (1996) *J Magn Reson* 122:9–15
29. Thiele H, Etstling J, Such P, Hofer P (1992) WinEPR. Bruker Analytic Gmb, Berlin
30. Weber RT (1995) WinEPR SimFonia. EPR Division, Bruker Instr. Inc., Billerica
31. Lund A, Shiotani M, Shimada S (2011) *Principles and applications of EPR spectroscopy*. Springer, New York
32. Abragam A, Bleaney B (1970) *Electron paramagnetic resonance of transition ions*. Clarendon Press, Oxford
33. Krzystek J, Ozarowski A, Telser J (2006) *Coord Chem Rev* 250:2308–2324
34. Benmelouka M, Tol JV, Borel A, Nellutla S, Port M, Helm L, Brunel LC, Merbach AE (2009) *Helv Chim Acta* 92:2173–2185
35. Caneschi A, Dei A, Gatteschi D, Massa CA, Pardi LA, Pousereau S, Sorace L (2003) *Chem Phys Lett* 371:694–699
36. Szyzewski A, Lis S, Kruczynski Z, But S (2002) *J Alloys Compd* 341:307–311
37. Szyzewski A, Krzyminiewski R, Lis S, Pietrzak J, Elbanowski M (1995) *Radiat Phys Chem* 45:935–938
38. Velchuri R, Kumar BV, Devi VR, Kumar KR, Prasad G, Virthal M (2009) *Spectrochim Acta A* 74:726–730
39. Velchuri R, Kumar BV, Devi VR, Prasad G, Prakash DJ, Virthal M (2011) *Mater Res Bull* 46:1219–1226
40. Zhou X, Westlund PO (2005) *Spectrochim Acta A* 62:76–82